Video Article

Facilitating Drug Discovery: An Automated High-content Inflammation Assay in Zebrafish

Christine Wittmann[1], Markus Reischl[2], Asmi H. Shah[1], Ralf Mikut[2], Urban Liebel[1,2], Clemens Grabher[1]

[1]Institute for Toxicology and Genetics, Karlsruhe Institute of Technology, Karlsruhe, Germany

[2]Institute for Applied Informatics, Karlsruhe Institute of Technology, Karlsruhe, Germany

Correspondence to: Clemens Grabher at clemens.grabher@kit.edu

Abstract

Zebrafish larvae are particularly amenable to whole animal small molecule screens[1,2] due to their small size and relative ease of manipulation and observation, as well as the fact that compounds can simply be added to the bathing water and are readily absorbed when administered in a <1% DMSO solution. Due to the optical clarity of zebrafish larvae and the availability of transgenic lines expressing fluorescent proteins in leukocytes, zebrafish offer the unique advantage of monitoring an acute inflammatory response *in vivo*. Consequently, utilizing the zebrafish for high-content small molecule screens aiming at the identification of immune-modulatory compounds with high throughput has been proposed[3-6], suggesting inflammation induction scenarios e.g. localized nicks in fin tissue, laser damage directed to the yolk surface of embryos[7] or tailfin amputation[3,5,6]. The major drawback of these methods however was the requirement of manual larva manipulation to induce wounding, thus preventing high-throughput screening. Introduction of the chemically induced inflammation (ChIn) assay[8] eliminated these obstacles. Since wounding is inflicted chemically the number of embryos that can be treated simultaneously is virtually unlimited. Temporary treatment of zebrafish larvae with copper sulfate selectively induces cell death in hair cells of the lateral line system and results in rapid granulocyte recruitment to injured neuromasts. The inflammatory response can be followed in real-time by using compound transgenic *cldnB::GFP/lysC::DsRED2*[6,9] zebrafish larvae that express a green fluorescent protein in neuromast cells, as well as a red fluorescent protein labeling granulocytes.

In order to devise a screening strategy that would allow both high-content and high-throughput analyses we introduced robotic liquid handling and combined automated microscopy with a custom developed software script. This script enables automated quantification of the inflammatory response by scoring the percent area occupied by red fluorescent leukocytes within an empirically defined area surrounding injured green fluorescent neuromasts. Furthermore, we automated data processing, handling, visualization, and storage all based on custom developed MATLAB and Python scripts.

In brief, we introduce an automated HC/HT screen that allows testing of chemical compounds for their effect on initiation, progression or resolution of a granulocytic inflammatory response. This protocol serves a good starting point for more in-depth analyses of drug mechanisms and pathways involved in the orchestration of an innate immune response. In the future, it may help identifying intolerable toxic or off-target effects at earlier phases of drug discovery and thereby reduce procedural risks and costs for drug development.

Video Link

The video component of this article can be found at https://www.jove.com/video/4203/

Protocol

1. Animal Handling

For the ChIn assay use 3 dpf larvae arising from group matings between homozygous double transgenic *cldnB::GFP/lysC::DsRED2* and *AB* (wild-type) fish. Collect embryos by natural spawning and raise them at 29 °C in E3 medium (5 mM NaCl, 0.17 mM KCl, 0.33 mM CaCl$_2$, 0.33 mM MgSO$_4$, and 0.1% methylene blue, equilibrated to pH 7.0) in Petri dishes. It is essential to maintain a density of embryos not exceeding 50-70 per plate.

2. Larva Sorting

Check all larvae under a fluorescence stereoscope for fluorescent reporter expression, spontaneous inflammation and appropriate age related development.

3. Screening Medium Preparation (Always prepare fresh)

Prepare E3 medium without methylene blue supplemented with DMSO (1% final) and MS222 (0.05 g/l).

4. CuSO4 Preparation (Always prepare fresh)

First weigh out $CuSO_4$ (M_r=159.6 g/mol) and prepare a 20 mM stock solution in dH_2O. Prepare 120 μM $CuSO_4$ working solution (from 20 mM stock solution) in E3/DMSO(1%)/MS-222. Protect $CuSO_4$ solution from light.

5. 384-well Plate Preparation (Greiner 384 Well Microplate)

Pre-add 20 μl of E3/DMSO(1%)/MS-222 to each well with a reverse pipette. An increased pipette tip bore is required to handle the embryos carefully without inflicting any wounding; this is done by cutting the tip to a 2 mm bore. Transfer single larva in 74 μl of medium to each well (84 μl for untreated control). If necessary, orient larvae in a lateral position within the well using a flexible Eppendorf Microloader Pipette Tip (Eppendorf; 5242 956.003).

Conduct all following liquid handling steps with a robot liquid handling workstation to ensure simultaneous treatment of all larvae.

6. Drug Treatment

Mix compounds in drug stock plate 5 times by pipetting up and down. Add 16 μl of 7.5X drug stock plate to each well and mix 5 times. Adjust tip position within wells to prevent injury of larvae and dispense the medium at 10 μl/s. Mix medium in wells 4 times to ensure homogenous distribution of the drug within the well.

7. Incubation

Incubate screening plate for 1 h at 29 °C covered with aluminum foil to protect compounds as well as $CuSO_4$ from light.

8. Chemical Wounding

Add 10 μl of 120 μM $CuSO_4$ working solution to each well except to negative controls, mix 4 times and incubate again for 1 h at 29 °C.

9. Washing

Remove and exchange 80 μl of medium from each well twice (in 20 μl steps) to remove compounds and $CuSO_4$.

10. Image Acquisition

Start image acquisition on an inverted automated microscope (i.e.: Olympus scan^R) 90 minutes after initial copper treatment. Set initial z-level so that neuromasts from right and left posterior lateral line are visible. Image each well once per hour in the channels brightfield, Cy3 and GFP in 4 focal planes (50 μm distance) using a 4x objective (N.A. = 0.13).

Additional information on image and data processing are available upon request.

11. Image Processing

1. Data sorting

Raw images are processed with our custom LabView software script. The first operation in the image processing pipeline is sorting of raw images from the microscope generated data folder by channel, well and time-point information.

2. Extended focus

Subsequently the software creates extended focus images from 4 focal planes for each of the channels.

3. RGB-overlay

In a last step the extended focus images from the 3 channels are merged to result in a final RGB-overlay image.

4. Automated neuromast detection

A pattern recognition tool (LabView Rapid IA prototyping tool) identifies neuromasts within the RGB overlay images and creates an empirically defined area of interest around the neuromasts.

5. Quantification

Within the empirically defined area of interest surrounding injured neuromasts red fluorescent leukocytes (reflected as red pixels) are scored resulting in a primary readout of percent area occupied by leukocytes (*Paol*). On average 95.27 ± 2.11% (FDA1) and 95.12 ± 1.56% (FDA2) of wells (larvae) have been detected properly and have subsequently been subjected to further data processing. The raw data output (*Paol* for each detected neuromast) is stored in a txt file and serves as the data input for the MATLAB scripts that process the raw data further.

12. Data Processing

1. *iMaps*

Assessing the success of individual experiments by graphical visualization of the raw data output *Paol* in a color code could be realized with so-called inflammation maps (*iMaps*) (**Figure 2**). Bright green reflects a high initial inflammatory index; black indicates no inflammation. This quick overview allows for rapid identification of failed experiments, which can then be excluded from further data analyses.

2. Averaging of controls

Each experimental plate contains 320 compounds reflecting a single data point per compound and time-point as well as 32 positive and negative controls, respectively. The 32 control replicates are averaged and standard deviation is calculated. For the controls only data points within 2 standard deviations are included.

3. Normalization

Normalization is done by spreadsheet analysis. The average value of DMSO, being the negative control, is set to 0 and the highest averaged *Paol* for the copper control is set to 1, so that the maximum difference between the positive and negative control is set to 1. Each compound's *Paol* is linearly interpolated or extrapolated to the respective controls on the experimental plate.

4. Final read-out: Inflammatory index

After sufficient replicate experiments (i.e. 15) have been conducted, normalized raw data from replicate experiments are averaged, resulting in a final read-out - the inflammatory index. The initial inflammatory index of the copper control starts at 100% for time-point zero and correlates to image acquisition start time (90 minutes after initial copper treatment).

5. Monotonic exponential regression fitting

Due to inflammation resolution over time we perform a monotonic exponential nonlinear regression fitting towards the initial inflammation by using $e^{(a_0+a_1 x)}$. a_0 is a measure for the initial response at t=0, a_1 is related to the slope of the magnitude over time.

6. 2-D feature space plot (Figure 4)

To generate the feature space, a non-linear regression is applied and a cluster-analysis divides the feature space into characteristic regions, thus allowing automated identification of interesting candidates from different immune-modulatory categories (anti-inflammatory, anti-resolution, pro-inflammatory, pro-resolution). All compounds are displayed in the 2-D plot based on the parameters a_0 and a_1.

13. Data Handling and Storage

Our data handling routines create webpages to visualize and represent such drug screens providing a quick overview of the image and data processing steps' results, as well as a detailed view when requested by the user[10]. Soft links to other relevant heterogeneous biological and chemical databases are integrated as well to provide a valuable resource for comparative and novel studies[11]. By these routines, proper data standards and metainformation are set for long term storage of this data.

14. Representative Results

In a pilot screen we analyzed a library consisting of 640 FDA approved known bioactive compounds for effects on initiation, progression or resolution of a granulocytic inflammatory response. Based on the observed effects we classified 4 types of immune modulatory phenotypes that may be indicative of different modes of action: anti-inflammatory (1), anti-resolution (2), pro-inflammatory (3) and pro-resolution (4), which can be described with the parameters a_0 and a_1, that arise from a monotonic non-linear regression fitting ($e^{a_0+a_1 x}$-)towards the initial inflammation. A_0 represents the magnitude of the inflammatory response whereas a_1 characterizes the slope of the curve and thus describes inflammation resolution. Displaying all compounds in a 2-D feature space plot (a_1 vs. a_0) allows for automated identification of hit candidates from the different immune modulatory categories (**Figure 3**).

45 out of 640 compounds exerted significant anti-inflammatory effect by reducing the initial inflammatory index to 50% or less. Within this category we found 6 compounds belonging to the pharmacological class of non-steroidal anti-inflammatory drugs (NSAIDs), confirming the validity of our approach. However, NSAIDs ranked not amongst the most potent anti-inflammatory drugs. Apart from the NSAIDs we found several additional pharmacological drug classes such as for example Angiotensin receptor blockers (ARBs), antibiotics and proton pump inhibitors.

7 compounds met the empirically defined threshold criteria for potential pro-resolution drugs.

18 drugs exerted a pro-inflammatory effect, resulting in exaggerated leukocyte recruitment to injured neuromasts compared to the positive controls.

Only 2 compounds prevented timely resolution of the inflammatory response.

The anti-inflammatory effect of several hit candidates (exemplary candidates from above mentioned pharmacological drug classes) from the pilot screen could be confirmed in a dose-dependent manner in subsequent secondary ChIn assays (data not shown). Retesting of 4 potential pro-resolution drugs did not confirm the indicated mode of action as exerted in the primary screen. 2 of the drugs had a slight anti-inflammatory potential at higher concentrations (20 µM). A third drug exhibited a marginal non-dose-dependent anti-inflammatory effect at drug concentrations ranging from 5 - 20 µM. The fourth drug had no effect on the inflammatory response at the concentrations tested.
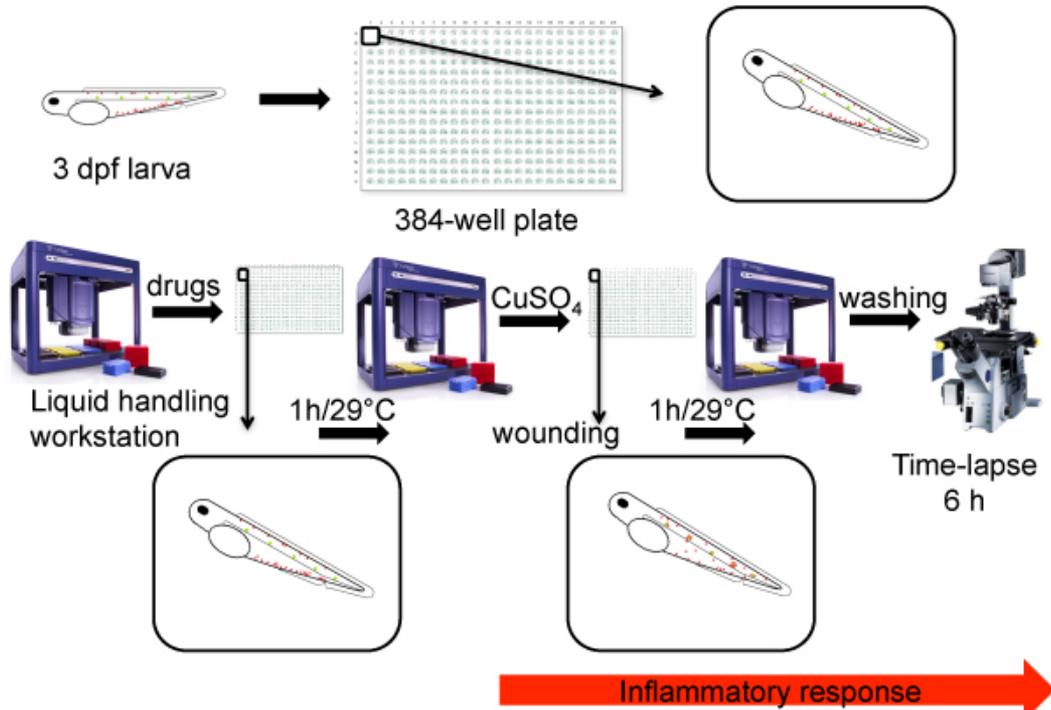

Figure 1. Workflow of the ChIn assay. Individual compound transgenic *cldnB::GFP/lysC::DsRED2* larvae (3 dpf) are manually distributed in 384-well microtiter plates. Drugs are added simultaneously to each well using a Zephyr Compact Liquid Handling Workstation. Assay plates are then incubated for 1 h at 29 °C. Treatment with $CuSO_4$- solution (10 µM final concentration) for 1 h inflicts the wounding and initiates an acute inflammatory response. Finally, copper solution and drugs are washed off and automated image acquisition is started (90 minutes after initial copper treatment).
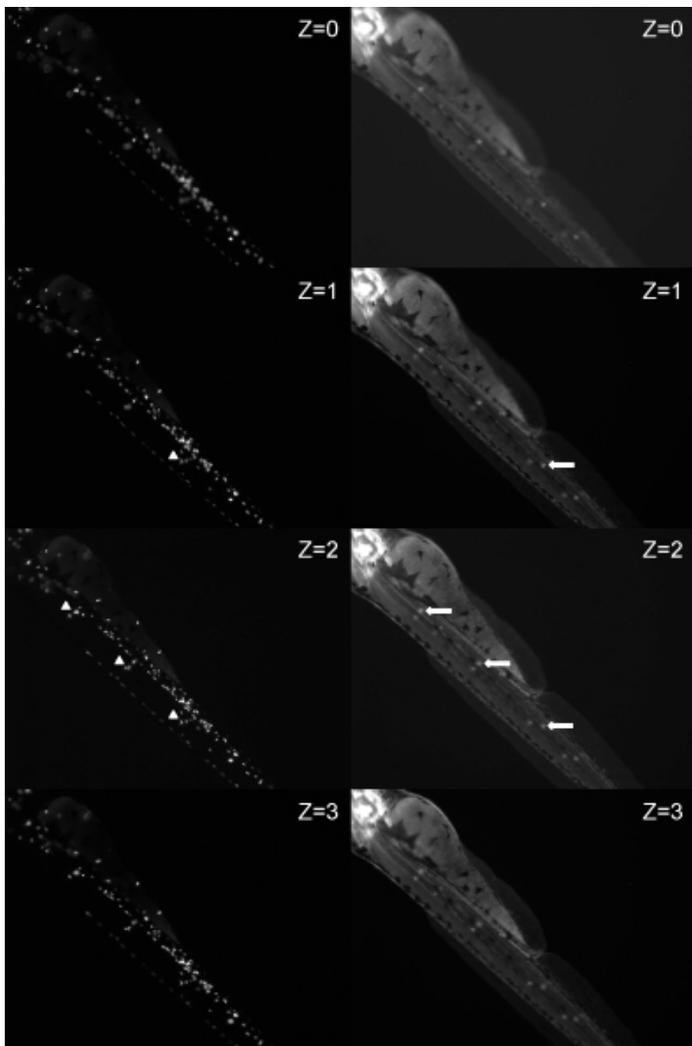
Figure 2. Overview picture of raw images. The figure shows raw images of 4 focal planes (Z=0 - 3) at distances of 50 µm in the channels Cy3 (left) and GFP (right), respectively. Arrows (Z=1,2) indicate exemplary neuromasts, arrowheads (Z=1,2) point to clustered leukocytes around neuromasts.
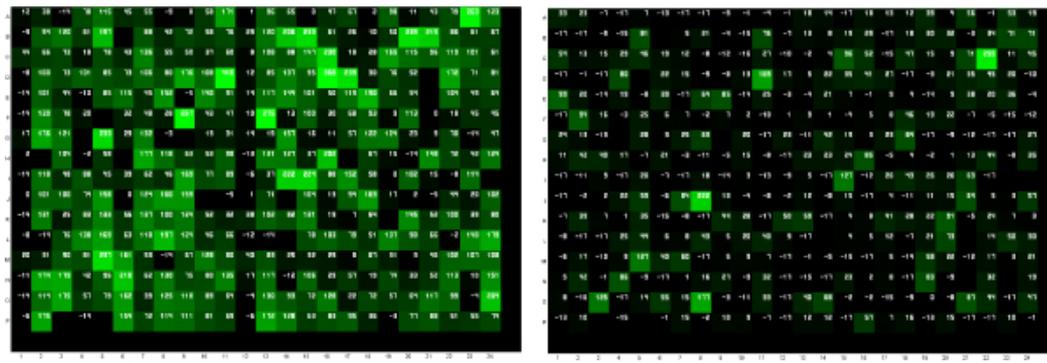

Figure 3. Inflammation Maps (iMaps). The success of individual experiments can be assessed in *iMaps* reflecting the inflammatory response (raw data) in a color code: Bright green reflects a high initial inflammatory response; black indicates no inflammation. *iMaps* at timepoint 0 (left) and time-point 5 (right) clearly show whether an experiment should be included in further data processing. Copper controls (row 13 and 24) show up in varying shades of green, whereas DMSO control wells (row 1 and 12) appear in dark green or black. At time-point 5, inflammation is almost resolved in copper controls, now indicated in dark shades of green or black. Click here to view larger figure.
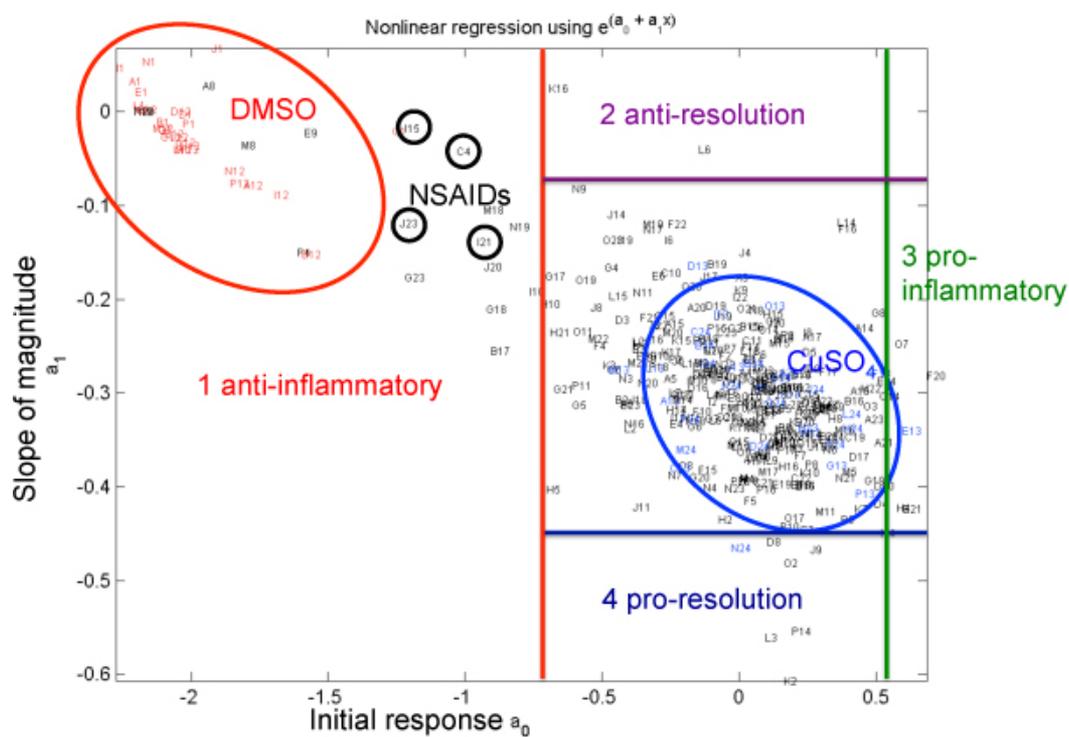
Figure 4. 2-D feature space plot of 320 compounds of an FDA approved library and their respective controls. All compound wells can be displayed in a 2-D feature space plot based on the parameters a_0 and a_1, which arise from a non-linear regression fitting ($e^{(a_0 + a_1 x)}$) towards the initial inflammation. This feature space plot allows automated identification of interesting candidates belonging to one of the following 4 immune-modulatory categories that may be indicative of the drugs' mode of action: anti-inflammatory (1), anti-resolution (2), pro-inflammatory (3) and pro-resolution (4). Click here to view larger figure.

Discussion

Here we present a fully automated high-throughput screening strategy enabling identification of immune-modulatory compounds in a whole animal context. Thus allowing monitoring of an acute inflammatory response *in vivo* and in real time.

We provide a protocol to apply zebrafish as a valuable model organism for drug discovery or drug repurposing efforts, since drug effects on leukocyte recruitment to wounds can be studied with relative ease in the context of a fully functional innate immune system. The unique advantage of our approach is the fact that chemical wounding renders manual larvae manipulation obsolete, thus permitting automation and screening in a high-throughput format.

Additionally, adverse or toxic drug effects as well as strong off-target effects can be easily assessed with the proposed set-up. The FDA approved library however did not contain any toxic compounds at the given screening concentrations. Nevertheless, we propose for apparent toxic compounds to compare the available dataset (e.g. immune modulatory phenotype, drug concentration) between members of the same pharmacological substance class present in the tested library. Toxic members of a substance family, that otherwise exerts a promising immune modulatory phenotype, could be retested at lower concentrations, if need be.

We have demonstrated the possibility of categorizing drugs automatically according to their exerted immune-modulatory effect. Drugs belonging to the category of anti-inflammatory compounds could be validated in independent experiments, most of the compounds exerting their effect in a dose-dependent manner. Four compounds identified as potential pro-resolution drugs could thus far not be confirmed as such. It also indicates that this particular immune modulatory category is difficult to describe, since no drugs solely affecting resolution have so far been described in literature. However, 3 of the 4 retested drugs showed an anti-inflammatory trend at higher molar concentrations. Optimizing the empirically defined threshold criteria should help to reduce the number of false-positives.

Furthermore, the presented technique offers the possibility to be utilized for the identification of mutations in genes affecting leukocyte migratory behavior[8].

Concluding, the proposed method can facilitate and accelerate drug discovery or drug repurposing efforts by yielding potential new lead structures with readily available information on drug tolerance, toxicity, dosage as well as potential off-target effects. Therefore, serving as a simple, cost- and time-saving strategy at early stages of drug development.

Disclosures

No conflicts of interest declared.

Acknowledgements

References

1. Peterson, R.T. & Fishman M.C. Discovery and use of small molecules for probing biological processes in zebrafish. *Methods Cell Biol.* **76**, 569 (2004).
2. Zon L.I. & Peterson, R.T. In vivo drug discovery in the zebrafish. *Nat. Rev. Drug. Discov.* **4** (1), 35-44 (2005).
3. Loynes, C.A., Martin, J.S., Robertson, A., Trushell, D.M., Ingham, P.W., Whyte, M.K., & Renshaw, S.A. Pivotal advance: pharmacological manipulation of inflammation resolution during spontaneously resolving tissue neutrophilia in the zebrafish. *J. Leukoc. Biol.* **87**, 203-12 (2009).
4. Martin, J.S. & Renshaw, S.A. Using *in vivo* zebrafish models to understand the biochemical basis of neutrophilic respiratory disease. *Biochem. Soc. Trans.* **37**, 830-837 (2009).
5. Renshaw, S.A., Loynes, C.A., Trushell, D.M., Elworthy, S., Ingham, P.W., & Whyte, M.K. A transgenic zebrafish model of neutrophilic inflammation. *Blood.* **108**, 3976-3978 (2006).
6. Hall, C., Flores, M.V., Storm, T., Crosier, K., & Crosier, P. The zebrafish lysozyme C promoter drives myeloid-specific expression in transgenic fish. *BMC Dev. Biol.* **7**, 42 (2007).
7. Redd, M.J., Kelly, G., Dunn, G., Way, M., & Martin, P. Imaging macrophage chemotaxis in vivo: studies of microtubule function in zebrafish wound inflammation. *Cell. Motil. Cytoskeleton.* **63**, 415-422 (2006).
8. D'Alençon, C.A., Peña, O.A., Wittmann, C., Gallardo, V.E., Jones, R.A., Loosli, F., Liebel, U., Grabher, C., & Allende, M.L. A high-throughput chemically induced inflammation assay in zebrafish. *BMC Biol.* **8**, 151, doi: 10.1186/1741-7007-8-151 (2010).
9. Haas, P. & Gilmour, D. Chemokine signaling mediates self-organizing tissue migration in the zebrafish lateral line. *Dev Cell.* **10**, 673-680 (2006).
10. Luetjohann, D.S., Shah, A.H., Christen, M.P., Richter F., Knese K., & Liebel, U. 'Sciencenet' - towards a global search and share engine for all scientific knowledge. *Bioinformatics.* **27**, 1734-1735 (2011).
11. Liebel, U., Kindler, B., & Pepperkok, R. 'Harvester': a fast meta search engine of human protein resources. *Bioinformatics.* **20**, 1962-1963 (2004).